COMPRESSED SENSING RADAR

Matthew Herman and Thomas Strohmer

Department of Mathematics, University of California, Davis, CA 95616-8633, USA
e-mail: {mattyh,strohmer}@math.ucdavis.edu

ABSTRACT

A stylized compressed sensing radar is proposed in which the time-frequency plane is discretized into an $N \times N$ grid. Assuming the number of targets K is small (i.e., $K \ll N^2$), then we can transmit a sufficiently "incoherent" pulse and employ the techniques of compressed sensing to reconstruct the target scene. A theoretical upper bound on the sparsity K is presented. Numerical simulations verify that even better performance can be achieved in practice. This novel compressed sensing approach offers great potential for better resolution over classical radar.

***Index Terms*—** Compressed sensing, radar, sparse recovery, system identification, Gabor analysis.

1. INTRODUCTION

Radar, sonar and similar imaging systems are in high demand in many civilian, military, and biomedical applications. The resolution of these systems is limited by classical time-frequency uncertainty principles. Using the concepts of compressed sensing (CS), we propose a radically new approach to radar, which under certain conditions provides better time-frequency resolution. In this simplified version of a monostatic, single-pulse radar system we assume that the targets are radially aligned with the transmitter and receiver. As such, we will only be concerned with the range and velocity of the targets. Future studies will include cross-range information.

Throughout this discussion we only consider functions with finite energy; that is, if $f \in L^2(\mathbb{R})$, then $\|f\|_2^2 = \int_{\mathbb{R}} |f(t)|^2 dt < \infty$. For two functions $f, g \in L^2(\mathbb{R})$, the *cross-ambiguity function* of $\tau, \omega \in \mathbb{R}$ is defined as

$$\mathcal{A}_{fg}(\tau,\omega) \;=\; \int_{\mathbb{R}} f(t+\tau/2)\overline{g(t-\tau/2)}\mathrm{e}^{-2\pi \mathrm{i}\omega t} dt \qquad (1)$$

where $\overline{\,\cdot\,}$ denotes complex conjugation, and the upright Roman letter $\mathrm{i} = \sqrt{-1}$. When $f = g$ we have the *(self) ambiguity function* $\mathcal{A}(\tau,\omega)$, and its shape $|\mathcal{A}(\tau,\omega)|$ above the time-frequency plane is called the *ambiguity surface*. The *radar uncertainty principle* [1] states that if

$$\iint_U |\mathcal{A}_{fg}(\tau,\omega)|^2 d\tau d\omega \;\geq\; (1-\varepsilon)\,\|f\|_2^2 \|g\|_2^2 \qquad (2)$$

for some *support* $U \subseteq \mathbb{R}^2$ and $\varepsilon \geq 0$, then $|U| \geq (1-\varepsilon)$.

In classical radar, the ambiguity function of f is the main factor in determining the resolution between targets [2]. Thus, the ability to identify two targets in the time-frequency plane is limited by the essential support of $\mathcal{A}_f(\tau,\omega)$ as dictated by the radar uncertainty principle. The main result of this paper is that, under certain conditions, CS radar achieves better target resolution than classical radar.

This work was partially supported by NSF Grant No. DMS-0511461 and NSF VIGRE Grant No. DMS-0135345.

2. COMPRESSED SENSING

Recently, the signal processing/mathematics community has seen a paradigmatic shift in the way information is represented, stored, transmitted and recovered [3, 4, 5]. This area is often referred to as *Sparse Representations and Compressed Sensing*. Consider a discrete signal $\boldsymbol{s}$ of length M. We say that it is K*-sparse* if at most $K \ll M$ of its coefficients are nonzero (perhaps under some appropriate change of basis). With this point of view the *true information* content of $\boldsymbol{s}$ lives in at most K dimensions rather than M. In terms of signal acquisition it makes sense then that we should only have to measure a signal $N \sim K$ times instead of M. We do this by observing N *non-adaptive, linear measurements* in the form of $\boldsymbol{y} = \boldsymbol{\Phi}\boldsymbol{s}$, where $\boldsymbol{\Phi}$ is a dictionary of size $N \times M$. If $\boldsymbol{\Phi}$ is sufficiently "incoherent," then the information of $\boldsymbol{s}$ will be embedded in $\boldsymbol{y}$ such that it can be perfectly recovered with high probability. Current reconstruction methods include using greedy algorithms such as *orthogonal matching pursuit* (OMP) [5], and solving the convex problem: $\min \|\boldsymbol{s'}\|_1$ such that $\boldsymbol{\Phi}\boldsymbol{s'} = \boldsymbol{y}$. The latter program is often referred to as *Basis Pursuit* (BP) [3, 4].

3. MATRIX IDENTIFICATION VIA CS

3.1. Problem Formulation

Consider an unknown matrix $\boldsymbol{H} \in \mathbb{C}^{N \times N'}$ and an orthonormal basis (ONB) $(\boldsymbol{H}_i)_i$ for $\mathbb{C}^{N \times N'}$. Note that there are necessarily NN' elements in this basis, and their ortho-normality is with respect to the Frobenius norm. Then there exist coefficients $(s_i)_i$ such that

$$\boldsymbol{H} \;=\; \sum_{i=0}^{NN'-1} s_i \boldsymbol{H}_i. \qquad (3)$$

Our goal is to identify/discover the coefficients $(s_i)_i$. Since the basis elements are fixed, identifying $(s_i)_i$ is tantamount to discovering $\boldsymbol{H}$. We will do this by designing a test function $\boldsymbol{f} = (f_0, \ldots, f_{N'-1})^{\mathrm{T}} \in \mathbb{C}^{N'}$ and observing $\boldsymbol{H}\boldsymbol{f} \in \mathbb{C}^N$. Here, $(\,\cdot\,)^{\mathrm{T}}$ denotes the transpose of a vector or a matrix. Figure 1 depicts this from a systems point of view where $\boldsymbol{H}$ is an unknown "block box." Systems like this are ubiquitous in engineering and the sciences. For instance, $\boldsymbol{H}$ may represent an unknown communications channel which needs to be identified for equalization purposes.

$$\boldsymbol{f} \longrightarrow \underset{\text{Black Box}}{\boxed{\;\boldsymbol{H}\;}} \longrightarrow \boldsymbol{y} = \boldsymbol{H}\boldsymbol{f}$$

Fig. 1. Unknown system $\boldsymbol{H}$ with input $\boldsymbol{f}$ and output observation $\boldsymbol{y}$.

For simplicity, from now on assume that $N' = N$. The observation vector can be reformulated as

$$\boldsymbol{y} \;=\; \sum_{i=0}^{N^2-1} s_i \boldsymbol{H}_i \boldsymbol{f} \;=\; \sum_{i=0}^{N^2-1} s_i \boldsymbol{\varphi}_i \;=\; \boldsymbol{\Phi s} \tag{4}$$

where the ith atom $\boldsymbol{\varphi}_i = \boldsymbol{H}_i \boldsymbol{f}$ is a column vector of length N, the concatenation of the atoms $\boldsymbol{\Phi} = (\, \boldsymbol{\varphi}_0 \,|\, \boldsymbol{\varphi}_1 \,|\, \cdots \,|\, \boldsymbol{\varphi}_{N^2-1}\,)$ is an $N \times N^2$ matrix, and $\boldsymbol{s} = (\, s_0,\, s_1,\, \cdots,\, s_{N^2-1}\,)^{\mathrm{T}}$ is a column vector of length N^2. The system of equations in (4) is clearly highly underdetermined. If $\boldsymbol{s}$ is *sufficiently sparse*, then there is hope of recovering $\boldsymbol{s}$ from $\boldsymbol{y}$. To use the reconstruction methods of CS we need to design $\boldsymbol{f}$ so that the dictionary $\boldsymbol{\Phi}$ is *sufficiently incoherent*.

3.2. The Basis of Time-frequency Shifts

It is well-known from pseudo-differential operator theory [1] that any matrix can be represented by a basis of **time-frequency shifts**. Let the $N \times N$ matrices $\boldsymbol{T}$ and $\boldsymbol{M}$ respectively denote the unit shift and modulation operators where $\boldsymbol{T}(f_0, \ldots, f_{N-2}, f_{N-1})^{\mathrm{T}} = (f_{N-1}, f_0, \ldots, f_{N-2})^{\mathrm{T}}$, $\boldsymbol{M} = \mathrm{diag}(\omega_N^0, \ldots, \omega_N^{N-1})$, and $\omega_N = \mathrm{e}^{2\pi \mathrm{i}/N}$ is the Nth root of unity. The ith time-frequency basis element is defined as $\boldsymbol{H}_i = \boldsymbol{M}^{i \bmod N} \cdot \boldsymbol{T}^{\lfloor i/N \rfloor}$ for $i = 0, \ldots, N^2 - 1$, where $\lfloor \cdot \rfloor$ is the floor function. Under this basis, it is known [6, 7] that some practical systems $\boldsymbol{H}$ with meaningful applications have a sparse representation $\boldsymbol{s}$.

A collection of vectors which are time-frequency shifts of a generating vector is called a *Gabor matrix* [1]. Without loss of generality assume $\|\boldsymbol{f}\|_2 = 1$. Since each $\boldsymbol{H}_i$ is a unitary matrix we have that $\|\boldsymbol{\varphi}_i\|_2 = 1$ for all i. We can also express $\boldsymbol{\Phi}$ as the concatenation of N blocks

$$\boldsymbol{\Phi} \;=\; \Big(\, \boldsymbol{\Phi}^{(0)} \,|\, \boldsymbol{\Phi}^{(1)} \,|\, \cdots \,|\, \boldsymbol{\Phi}^{(N-1)} \Big) \tag{5}$$

where the kth block $\boldsymbol{\Phi}^{(k)} = \boldsymbol{D}_k \cdot \boldsymbol{W}_N$ is composed of $\boldsymbol{D}_k = \mathrm{diag}(f_k, \ldots, f_{N-1}, f_0, \ldots, f_{k-1})$ and $\boldsymbol{W}_N = (\omega_N^{pq})_{p,q=0}^{N-1}$.

3.3. The Coherence of a Dictionary

We are interested in how the atoms of a general dictionary $\boldsymbol{\Phi} = (\boldsymbol{\varphi}_i)_i \in \mathbb{C}^{N \times M}$ (with $N \le M$) are "spread out." This can be quantified by examining the magnitude of the inner product between its atoms. The *coherence* $\mu(\boldsymbol{\Phi})$ is defined as the maximum of all of the distinct pairwise comparisons $\mu(\boldsymbol{\Phi}) = \max_{i \neq i'} |\langle \boldsymbol{\varphi}_i, \boldsymbol{\varphi}_{i'} \rangle|$. Assuming each $\|\boldsymbol{\varphi}_i\|_2 = 1$, the mutual coherence is bounded [8] by

$$\sqrt{\frac{M-N}{N(M-1)}} \;\le\; \mu(\boldsymbol{\Phi}) \;\le\; 1. \tag{6}$$

When a dictionary can be expressed as the union of 2 or more ONBs, this lower bound becomes $1/\sqrt{N}$ [9].

3.4. The Probing Test Function $\boldsymbol{f}$

We now introduce a candidate probe function $\boldsymbol{f}$ which results in remarkable incoherence properties for the dictionary $\boldsymbol{\Phi}$. Consider the *Alltop sequence* $\boldsymbol{f}_{\mathrm{A}} = (f_n)_{n=0}^{N-1}$ for some prime $N \ge 5$ where [10]

$$f_n \;=\; \frac{1}{\sqrt{N}}\, \mathrm{e}^{2\pi \mathrm{i} n^3/N}. \tag{7}$$

Let $\boldsymbol{\Phi}_{\mathrm{A}}$ denote the Gabor matrix generated by the Alltop sequence (7). Since its atoms are already grouped into $N \times N$ blocks in (5), we will maintain this structure by denoting the jth atom of the kth block as $\boldsymbol{\varphi}_j^{(k)}$. Within the *same* block (i.e., $k = k'$) we have

$$\textbf{Property 1:} \qquad |\langle \boldsymbol{\varphi}_j^{(k)}, \boldsymbol{\varphi}_{j'}^{(k)} \rangle| \;=\; \begin{cases} 0, & \text{if } j \neq j' \\ 1, & \text{if } j = j'. \end{cases}$$

Thus, each $\boldsymbol{\Phi}^{(k)}$ is an ONB for $\mathbb{C}^N$. Moreover, for *different* blocks (i.e., $k \neq k'$) we have

$$\textbf{Property 2:} \qquad |\langle \boldsymbol{\varphi}_j^{(k)}, \boldsymbol{\varphi}_{j'}^{(k')} \rangle| \;=\; \frac{1}{\sqrt{N}}$$

for all $j, j' = 0, \ldots, N-1$. This means that there is a *mutual incoherence* between the atoms of different blocks. Trivially, it follows that $\mu(\boldsymbol{\Phi}_{\mathrm{A}}) = 1/\sqrt{N}$. Furthermore, with $M = N^2$ in (6) we see that the lower bound of $1/\sqrt{N+1}$ is practically attained! (See [11] for more details on this and on equiangular line sets.)

3.5. Identifying Matrices via CS: Theory

Having established the incoherence properties of the dictionary $\boldsymbol{\Phi}_{\mathrm{A}}$ we can now move on to apply the concepts and techniques of CS. It is worth pointing out that most CS scenarios deal with a K-sparse signal $\boldsymbol{s}$ (for some *fixed* K), and one is tasked with determining how many observations are necessary to recover the signal. Our situation is markedly different. Due to the fact that $\boldsymbol{\Phi}_{\mathrm{A}}$ is constrained to be $N \times N^2$, we know $\boldsymbol{y} = \boldsymbol{\Phi}_{\mathrm{A}} \boldsymbol{s}$ we will contain exactly N observations. With N fixed, our CS dilemma is to determine how sparse $\boldsymbol{s}$ should be such that it can be recovered from $\boldsymbol{y}$. We hope to recover any K-sparse signal for $K \le C \cdot N/\log N$ for some $C > 0$. The following two theorems [11] summarize the recovery of matrices via CS when identified with the Alltop sequence with prime $N \ge 5$.

Theorem 1. *Suppose $\boldsymbol{H} = \sum_i s_i \boldsymbol{H}_i \in \mathbb{C}^{N \times N}$ has a K-sparse representation under the time-frequency ONB, with $K < \frac{1}{2}(\sqrt{N} + 1)$, and that we have observed $\boldsymbol{y} = \boldsymbol{H} \boldsymbol{f}_{\mathrm{A}}$. Then we are* ***guaranteed*** *to recover $\boldsymbol{s}$ either via BP or OMP.*

The sparsity condition in Theorem 1 is rather strict. Instead of the requirement of *guaranteed* perfect recovery, we can ask to achieve it with only *high probability*. This more modest expectation provides us with a much more realistic sparsity condition.

Theorem 2. *Suppose random $\boldsymbol{H} = \sum_i s_i \boldsymbol{H}_i \in \mathbb{C}^{N \times N}$ has a K-sparse representation under the time-frequency ONB where $K \le N/16 \log(N/\varepsilon)$ with $\varepsilon \le 1/\sqrt{2}$, and that we have observed $\boldsymbol{y} = \boldsymbol{H} \boldsymbol{f}_{\mathrm{A}}$. Then BP will recover $\boldsymbol{s}$ with probability greater than $1 - 2\varepsilon^2 - K^{-\vartheta}$ for some $\vartheta \ge 1$ s.t. $\sqrt{\vartheta \log N / \log(N/\varepsilon)} \le c$ where c is an absolute constant.*

3.6. Identifying Matrices via CS: Simulation

Numerical simulations were performed and indicate that the theory above is actually somewhat pessimistic. The simulations were conducted as follows. The values of prime N ranged from 5 to 127, and $1 \le K \le N$. For each ordered pair (N, K) a K-sparse vector $\boldsymbol{s}$ of length N^2 was randomly generated. The nonzero locations were chosen from a uniform distribution, and their magnitudes were independently chosen from a Gaussian distribution of zero mean and unit variance. With this random $\boldsymbol{s}$ the observation $\boldsymbol{y} = \boldsymbol{\Phi}_{\mathrm{A}} \boldsymbol{s}$ was generated. Then, $\boldsymbol{y}$ and $\boldsymbol{\Phi}_{\mathrm{A}}$ were input to a linear program [12] to solve $\min \|\boldsymbol{s}'\|_1$ s.t. $\boldsymbol{\Phi}_{\mathrm{A}} \boldsymbol{s}' = \boldsymbol{y}$. This procedure was repeated 15 times and averaged.

Figure 2 shows how the numerical simulations compare to Theorems 1 and 2. The error $\|\boldsymbol{s} - \boldsymbol{s}'\|_2$ as a function of (N, K) is shown as solid, gray-black contour lines. The dashed, red line represents $K = N/\log N$. The zone of "perfect reconstruction" lies *below* this line. In this region random $N \times N$ matrices with $1 \leq K \leq N/\log N$ nonzero entries can be perfectly recovered with high probability. This is empirical evidence that the denominator of K in Theorem 2 can be relaxed from $\log(N/\varepsilon)$ to just $\log N$ as desired. However, it is still an open mathematical problem to prove this for the Alltop sequence. Note also, the proportionality constant is *exactly* unity here. Furthermore, the overly strict constraint of Theorem 1 can be seen by the lower dash-dotted, blue line representing $K = \frac{1}{2}(\sqrt{N} + 1)$.

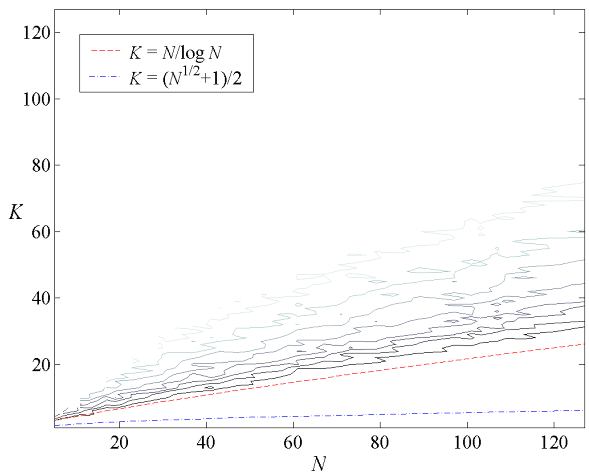

Fig. 2. Matlab simulation solving: $\min \|\boldsymbol{s}'\|_1$ s.t. $\boldsymbol{\Phi}_{\mathrm{A}}\boldsymbol{s}' = \boldsymbol{\Phi}_{\mathrm{A}}\boldsymbol{s}$.

4. RADAR

4.1. Classical Radar Primer

Consider the following simple (narrowband) 1-dimensional, monostatic, single-pulse radar model. Suppose a target located at *range* x is traveling with *constant velocity* v and has *reflection coefficient* s_{xv}. After transmitting signal $f(t)$, the receiver observes the reflected signal

$$r(t) \;=\; s_{xv} f(t - \tau_x) \mathrm{e}^{2\pi \mathrm{i} \omega_v t}, \tag{8}$$

where $\tau_x = 2x/c$ is the round trip time of flight, c is the speed of light, $\omega_v \approx -2\omega_0 v/c$ is the Doppler shift, and ω_0 is the carrier frequency. The basic idea is that the *range-velocity* information (x, v) of the target can be inferred from the observed *time delay-Doppler shift* (τ_x, ω_v) of f in (8). Hence, a time-frequency shift basis is a natural representation for radar systems.

Using a matched filter at the receiver, the magnitude of the cross-ambiguity function (1) between r and f is calculated

$$\begin{aligned} |\mathcal{A}_{rf}(\tau, \omega)| \;&=\; \left| \int_{\mathbb{R}} r(t) \overline{f(t - \tau)} \mathrm{e}^{-2\pi \mathrm{i} \omega t} dt \right| \\ &=\; \left| s_{xv} \mathcal{A}_f(\tau - \tau_x, \omega - \omega_v) \right| \end{aligned} \tag{9}$$

From this we see that the time-frequency plane consists of the ambiguity surface of f *centered at the target's "location"* (τ_x, ω_v). Extending (9) to include multiple targets is straightforward. Targets which are too close will have overlapping ambiguity functions and this may blur the exact location of the targets, or how many there are in a given region of the time-frequency plane.

4.2. CS Radar

We now propose our stylized CS radar which under appropriate conditions can "beat" the classical uncertainty principle! Consider K targets with unknown range-velocities and corresponding reflection coefficients. Next, discretize the time-frequency plane into an $N \times N$ grid so that the targets lie on the grid-points. Recognizing that each point on the grid represents a unique time-frequency shift $\boldsymbol{H}_i$, it is easy to see that each possible combination of target scenes can be represented by some matrix $\boldsymbol{H}$ as in (3). If the number of targets $K \ll N^2$, then the time-frequency grid will be sparsely populated. By "vectorizing" the grid, we can represent it as an $N^2 \times 1$ **sparse vector** $\boldsymbol{s}$. Assume that the Alltop sequence is sent by the transmitter[1]. If the number of targets obey the sparsity constraints in Theorems 1 and 2, then we will be able to reconstruct the original target scene using CS techniques.

4.3. CS and Classical Radar Simulations

Figure 3 shows the result of Matlab radar simulations. For purposes of normalization the grid spacing in these figures is $1/\sqrt{N}$. Hence, the numbers shown on the axes represent multiples of $1/\sqrt{N}$. A random time-frequency scene with $K = 10$ targets and $N = 47$ is presented in Figure 3(a). Targets which are darker indicate a larger reflection coefficient. The CS radar simulation [12] used the Alltop sequence to identify the targets. In Figure 3(b) it is clear that CS was able to *perfectly reconstruct* the target scene when there was no added noise (note, $K \leq N/\log N$ was satisfied). Based on the grid of the discretized time-frequency plane in these figures it is obvious that we can resolve targets located at *adjacent grid points*. Thus, **CS radar has a resolution of** $1/2\sqrt{N}$.

Figure 3(d) illustrates how CS starts to suffer in the presence of 15 dB of additive white Gaussian noise (AWGN). Some faint false positives have appeared, yet the target scene has still been identified. Moreover, the two closest targets in the center are resolved while traditional radar techniques may fail in this scenario. The performance of CS radar in the presence of 5 dB AWGN (not shown, see [11]) was somewhat worse. Several targets were lost and there were many false positives. It remains an open problem in the CS community how to deal with such noisy situations.

Figures 3(c) and 3(e) show the original target scene reconstructed when probed with a Gaussian pulse. The ambiguity function associated with a Gaussian pulse is a 2D Gaussian pulse. Therefore, according to (9) we see that the radar scenes in these figures consist of a 2D Gaussian pulse centered at each target in the time-frequency plane. It is clear that some of the targets are contained within the Heisenberg boxes of neighboring targets. Depending on the sophistication of subsequent algorithms some of the targets (e.g., the two closest in the center) may be unresolvable.

As a consequence of the grid spacing, the Heisenberg box associated with the Gaussian pulse's ambiguity surface has been normalized to a square of unit area. This is empirically verified in Figures 3(c), and 3(e) where we see that the diameter of the uncertainty region around each target spans approximately seven grid points. Since the grid spacing is $1/\sqrt{N}$ we confirm that the base and height of the Heisenberg box are each approximately $7/\sqrt{47} \approx 1$.

[1] The transmitter sends *analog* signals. We assume here that there exists a continuous signal which when discretized is the Alltop sequence (7).

Therefore, we have a rough measure of the target resolution of a Gaussian pulse: here **classical radar yields a resolution of** $1/2$. Comparing the resolution of classical radar with that of CS we see that $1/2 > 1/2\sqrt{N}$ for $N \geq 2$. Thus, we claim that CS radar can achieve better resolution than classical radar. Moreover, by increasing N the time-frequency plane will be discretized into a finer grid and this will increase CS's resolution. Of course, there are practical limits on how large N can be (refer to the Discussion section).

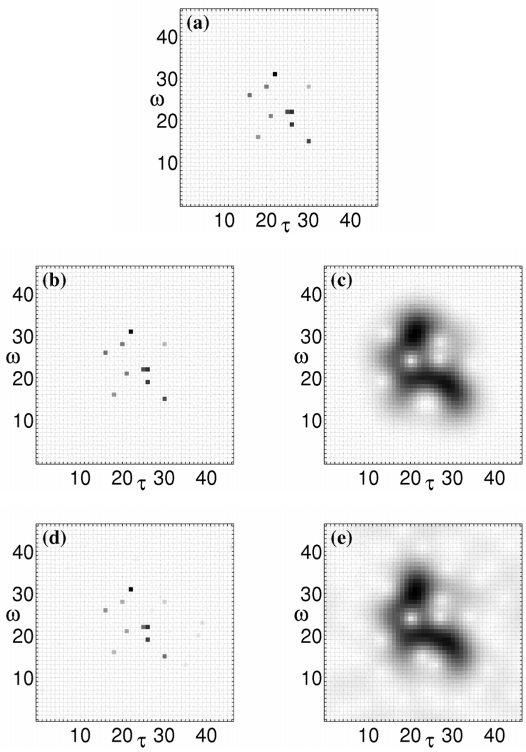

Fig. 3. Radar simulation. (a) Original target scene. Reconstruction with no noise: (b) CS and (c) Classical radar. Reconstruction with 15dB AWGN: (d) CS and (e) Classical radar.

5. DISCUSSION

We have provided a sketch for a high-resolution radar system based on CS. It must be stressed that our model presents radar in an overly simplified manner. In reality, radar engineers employ highly sophisticated methods to identify targets. For example, rather than a single pulse, a signal with multiple pulses is often used and information is averaged over several observations. In particular, the results in Figures 3(c) and 3(e) are included only for rough comparison. Since many of the implementation details of our CS radar have yet to be determined, and since classical radar can also be implemented in many ways we were unable to make a completely conclusive comparison between their respective resolutions. Regardless, the classical radar uncertainty principle lies at the core of traditional approaches and limits their performance. We contend that CS provides the potential to achieve higher resolution between targets.

We also did not address how to discretize the analog signals used in both CS and classical radar. A more detailed study addressing these issues is the topic of another paper. Related to the discretization issue is the fact that CS radar does not use a matched filter at the receiver. This will directly impact analog to digital conversion, and has the potential to reduce the overall data rate. These matters are discussed in the paper of Baraniuk and Steeghs [13], although they do not address the case of moving targets.

The success of this stylized CS radar relied on the incoherence of the dictionary $\mathbf{\Phi}_{\mathrm{A}}$ resulting from the Alltop sequence. There exist other probing functions with similar incoherence properties. Numerical simulations with $\boldsymbol{f}$ as a random Gaussian signal, as well as a constant-envelope random-phase signal indicate similar behavior to what we have reported for the Alltop sequence. At the time of writing this paper, we became aware of a similar study by Pfander, Rauhut and Tanner [14] where they examine some of these issues.

Narrowband radar is by no means the only application to which the techniques presented here can be used. *Wideband* radar admits a received signal which is well-represented by a wavelet basis, and the dictionary $\mathbf{\Phi}$ could be reformulated accordingly. There are also applications to many other linear time-varying systems such as sonar, estimation of underwater acoustic communication channels [7], and blind source separation.

6. REFERENCES

[1] K. Gröchenig, *Foundations of time-frequency analysis*. Boston: Birkhäuser, 2001.

[2] A. W. Rihaczek, *High-Resolution Radar*. Boston: Artech House, 1996, (originally published: McGraw-Hill, NY, 1969).

[3] D. L. Donoho, "Compressed sensing," *IEEE Trans. Inf. Theory*, vol. 52, no. 4, pp. 1289–1306, 2006.

[4] E. J. Candès, J. Romberg, and T. Tao, "Robust uncertaitny principles: Exact signal reconstruction from highly incomplete frequency information," *IEEE Trans. Inf. Theory*, vol. 52, no. 2, pp. 489–509, Feb. 2006.

[5] J. A. Tropp, "Greed is good: Algorithmic results for sparse approximation," *IEEE Trans. Inf. Theory*, vol. 50, no. 10, pp. 2231–2242, Oct. 2004.

[6] P. A. Bello, "Characterization of randomly time-variant linear channels," *IEEE Trans. on Comm.*, vol. 11, no. 4, pp. 360–393, Dec. 1963.

[7] W. Li and J. C. Preisig, "Estimation and equalization of rapidly varying sparse acoustic communication channels," *Proc. IEEE OCEANS 2006*, pp. 1–6, Sept. 2006.

[8] L. R. Welch, "Lower bounds on the maximum cross-correlation of signals," *IEEE Trans. Inf. Theory*, vol. 20, no. 3, pp. 397–399, 1974.

[9] P. Delsarte, J. M. Goethals, and J. J. Seidel, "Bounds for systems of lines and Jacobi poynomials," *Philips Res. Repts*, vol. 30, no. 3, pp. 91^*–105^*, 1975.

[10] W. O. Alltop, "Complex sequences with low periodic correlations," *IEEE Trans. Inf. Theory*, vol. 26, no. 3, pp. 350–354, May 1980.

[11] M. Herman and T. Strohmer, "High-resolution radar via compressed sensing," *Sub. to IEEE Trans. Sig. Proc.*, Oct. 2007.

[12] M. Grant, S. Boyd, and Y. Ye, "cvx: Matlab software for disciplined convex programming." [Online]. Available: `http://www.stanford.edu/~boyd/cvx/`

[13] R. Baraniuk and P. Steeghs, "Compressive radar imaging," *Proc. 2007 IEEE Radar Conf.*, pp. 128–133, Apr. 2007.

[14] G. E. Pfander, H. Rauhut, and J. Tanner, "Identification of matrices having a sparse representation," preprint June 2007.